

Radiation Pressure on a Free Liquid Surface

A. Ashkin and J. M. Dziedzic

Bell Telephone Laboratories, Holmdel, New Jersey 07733

(Received 10 November 1972)

The force of radiation pressure on the free surface of a transparent liquid dielectric has been observed using focused pulsed laser light. It is shown that light on either entering or leaving the liquid exerts a net outward force at the liquid surface. This force causes strong surface lens effects, surface scattering, and nonlinear absorption. The data relate to the understanding of the momentum of light in dielectrics.

We report the observation of the forces of radiation pressure from a focused pulsed laser beam on the free surface of a lossless liquid dielectric medium. We find that light on either entering or leaving the liquid exerts a net outward force at the surface of the dielectric medium. This force causes surface motion which results in strong surface lens effects, strong surface scattering, and nonlinear absorption. This result has bearing on the momentum of light in dielectric media, the ponderomotive force of electromagnetic waves in dielectric media, and the self-focusing of laser light in liquids. Light on entering a dielectric from free space has its momentum changed because of Fresnel reflection and by interaction with the medium. If p_0 is the momentum in free space and p the momentum in the medium of refractive index n , the net change in momentum is $p_0(1+R) - p(1-R)$, where R is the Fresnel reflection coefficient. This difference must be balanced by a mechanical force on the medium. On this basis, J. J. Thomson and Poynting¹ concluded that light on entering a dielectric exerts a net outward force at the surface. For the momentum in the medium they used $p = Un/c$, where U is the energy. This simply replaces c by c/n in the free-space momentum $p_0 = U/c$. Over the years there has been controversy over the proper form of the momentum of light in dielectrics.² Apart from Un/c , which is the so-called Minkowski value, there is U/cn proposed by Abraham. Recently, Burt and Peierls³ gave arguments in favor of Abraham's value in agreement with other recent work.⁴ Using $p = U/cn$ they predict that light should exert a net inward force on a dielectric interface. They also fail to understand the measurement of Jones and Richards⁵ of the light force on a metal vane in liquid, which agrees with $p = Un/c$. The existence of these disparate views on the direction of the surface force prompted the present experiment.⁶ Also, radiation pres-

sure on a dielectric discontinuity has served as the basis of numerous other *Gedankenexperimente*.⁷ Kats and Kontorovich⁸ considered the effect of laser light on liquid surfaces in connection with nonlinear effects and suggest that surface lenses can be made comparable with the nonlinear lenses generated in self-focusing experiments.

In our experiment we have generated surface lenses free of background thermal or nonlinear index changes. This was accomplished using 20 pulses per second of single transverse-mode doubled neodymium:yttrium-aluminum-garnet radiation at $\lambda = 0.53 \mu\text{m}$ having a peak power of 1-4 kW and a width τ of 60 nsec focused to a spot diameter of $2w_0 = 4.2 \mu\text{m}$ on the surface of water. Water should give low thermal lens effects⁹ for $\lambda = 0.53 \mu\text{m}$ since absorption is low ($\alpha \approx 3 \times 10^{-4} \text{ cm}^{-1}$ and two-photon absorption is negligible), dn/dT is lower than most liquids, and finally the light pulse width is less than the thermal time constant which reduces thermal lensing by ~ 70 . Since our power of 4 kW is well below the threshold for self-focusing¹⁰ ($\sim 1 \text{ MW}$), nonlinear lens effects should be minimal. With 4 kW and a 4.2- μm spot diameter we expect a force sufficient to overcome surface tension and give surface motion. For the surface tension force we use $2\pi rS \times \sin\theta$, where r is the beam radius to the half-power point, S the surface tension, and θ the angle of the surface normal and the beam. This has a maximum value $\sim 5 \times 10^{-2} \text{ dyn}$ for $\theta = 90^\circ$ using $r = 1.2 \mu\text{m}$. With 4 kW and using either Un/c or U/cn for p , the radiation pressure force is $\sim 4 \times 10^{-1} \text{ dyn}$ which exceeds surface tension by a factor of 8. This force is also 10^3 - 10^4 larger than needed to move or support micrometer-size free particles.¹¹

Figure 1 shows the apparatus for studying laser-induced lenses. Light is focused on the water surface from above and viewed from below with a microscope and scanning slit-detector

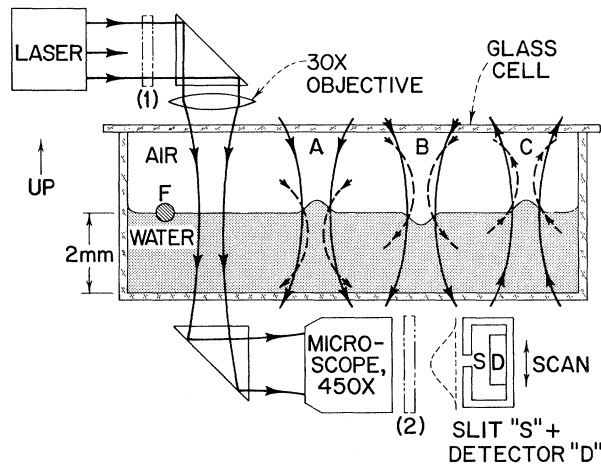


FIG. 1. Basic apparatus: A, Beam shapes for low power (solid curve) and high power (dashed curve) for positive surface lens; B, shapes (for low and high power) for a negative surface lens. For A and B the beam is incident from above. C, beam shapes for low and high power for a positive surface lens with the beam incident from below.

combination. To identify the surface with the microscope we floated a glass fiber F , $2-4 \mu\text{m}$ in diameter, as a local reference. Damage to the optics was avoided with long-working-distance objectives. The beam shapes were recorded at various planes above and below the surface at low and high power. To change the power level an attenuator was moved from position (1) in front of the laser to position (2) in front of the detector. Using a boxcar integrator with a 10-nsec gate we could measure the beam shapes at different times during the light pulse and thus follow the time development of the lens. If the force is outward on entering the liquid, the surface should lift up and form a positive or focusing lens which changes the beam shape at high power as shown at A in Fig. 1. If the force is inward, the surface should depress forming a negative lens as at B in Fig. 1. The beam shapes observed at high power will be the real beam shapes when viewed below the surface lens and virtual shapes when viewed above the lens. Figure 2 shows results for the beam shapes taken with 3 kW of power when measured ~ 250 nsec after the peak of the light pulse. The data show strong lens effects at high power. The data suggest a positive lens at the upper crossover as at A in Fig. 1. From data taken at other times we get the time development of the lens shown in Fig. 3(b). The light pulse shape is shown in Fig. 3(a). In Fig. 3(b) the lens strength is taken as

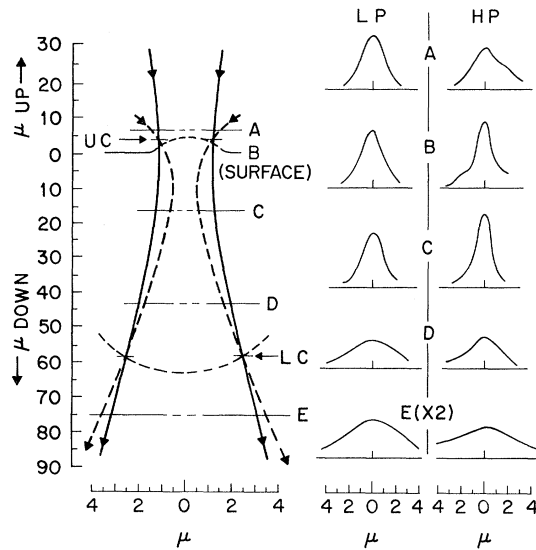


FIG. 2. Left, observed beam shapes at the half-power points, at low power (LP) (solid curve) and high power (HP) (dashed curve). A positive lens is dashed in at the upper crossover UC. A negative lens is dashed in at the lower crossover LC. Right, detailed scans of shapes, i.e., power versus position, at the indicated planes.

the reciprocal of the focal length of the ideal positive lens which best fits the observed beam shape. We see that the lens develops strongly hundreds of nanoseconds after the peak of the light pulse. At these times the light intensity, though weak, is adequate to study the lens shape. We show that the time development of the lens and the surface displacement can only be reason-

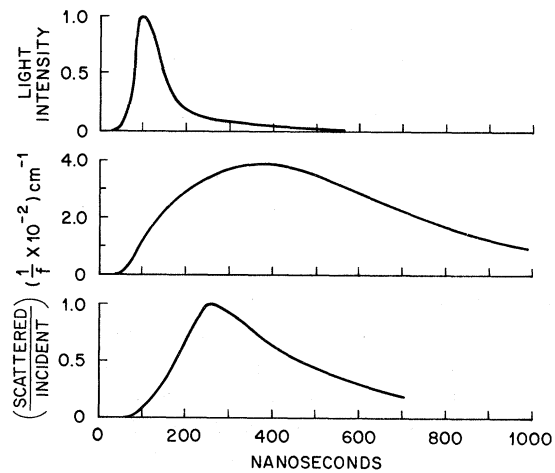


FIG. 3. Time development of (a) light pulse, (b) lens strength in units of $1/f$ (cm^{-1}), where f is the focal length, and (c) normalized scattering, i.e., (scattered light)/(incident light).

ably understood in terms of a positive lens located $\sim 4 \pm 2 \mu\text{m}$ above the original surface at the upper crossover UC of Fig. 2. Assuming the force is on for only $t = \tau = 60 \text{ nsec}$, the liquid receives an impulse $\int F dt \cong 1.8 \times 10^{-8} \text{ dyn sec}$. If we take a mass $= 1.5 \times 10^{-11} \text{ g}$, which is reasonable for a lens at the upper crossover, this results in a velocity $v \cong 1.2 \times 10^3 \text{ cm/sec}$ and a surface displacement $d \cong 0.4 \mu\text{m}$ after time τ . Subsequently, the moving mass coasts upward to a stop restrained only by surface tension (i.e., $\int 2\pi r S dt = \int F dt$). Thus, after a time of 390 nsec the lens has moved up to $d \cong 2.5 \mu\text{m}$ and is fully developed. The lens should then relax as a result of the continuing pull of surface tension after another 660 nsec, i.e., at $t \cong 1000 \text{ nsec}$. Thus, these semiquantitative considerations agree with a positive lens in Fig. 2 and the time dependence of Fig. 3(b). Even the strength of the lens is reasonable. To get the 20- μm average focal length observed in Fig. 2, we need a lens with an average radius of curvature $\sim 5 \mu\text{m}$. If we try now to interpret the data of Fig. 2 in terms of a negative lens at the lower crossover, then because of the larger mass involved we get discrepancies between the calculated and observed displacements of $\sim 10^4$. We also experimentally ruled out a negative lens at the lower crossover. If we raise the power to $\sim 4 \text{ kW}$ this increases the lens strength, and we find that the upper and lower crossovers both move up. This is only consistent with the surface located at the upper crossover. Similarly for weaker lenses both the upper and lower crossovers move down.

We have thus far attributed the observed lenses to surface deformation and given reasons for expecting negligible thermal and nonlinear lens effects. We also showed this experimentally by looking for lenses when the laser was focused $\sim 500 \mu\text{m}$ into the depth of the water. Here thermal and nonlinear lens effects, if present, should still occur, whereas surface lens effects should disappear. We found no detectable lenses.

Finally, we irradiated the free surface from below, i.e., from within the liquid. We find that the surface has again lifted up to form a positive lens as indicated at C in Fig. 1. This is as expected since if light on entering a dielectric medium exerts an outward force on the entering surface, it must also exert an outward force on the exiting surface to maintain the momentum balance.

Another feature accompanying strong lens development is the appearance of strong surface light scattering. This is seen at all angles, but

mostly as a broad halo in the forward direction. Scattering is also evident in Fig. 2 where the integrated intensity at high and low powers can often differ by 20%. This lost power is the scattered light. We expect some scattering and beam-shape distortions from a smooth nonideal lens of small radius of curvature. However, we attribute most of the large-angle scattering at higher powers to finer scale ripples or possibly some necking in of the lens due to incipient droplet formation. Figure 3(c) shows the time development of the scattering. This differs from the lens development indicating a different origin. Surface scattering provides another method of determining the position of the lens. Since the scattering source must lie at the surface within the core of the beam, we located with the microscope the depth at which the scattered halo shrinks into the beam core. This occurs as expected at the upper crossover and *not* at the lower crossover. Also, by viewing the scattering at grazing incidence above and below the surface, we observe that the intensity falls almost to zero as the angle below the surface decreases to a few degrees, whereas the intensity increases somewhat as the grazing angle decreases from above. This is understood from the reflecting and transmitting properties of a surface only if the scattering source is located *above* the background surface. Thus, this gives an independent determination of the position of the surface at high power.

The presence of surface motion implies the existence of a nonlinear optical energy loss for transparent dielectrics since the kinetic energy of the moving liquid is eventually lost to heat. In our experiment it represents a fractional energy loss of $\sim 10^{-8}$. This varies as the impulse squared. At higher impulses we eventually expect droplets a few micrometers in diameter will be ejected from the surface at considerable velocity. With lower surface tension all effects should occur more strongly. Indeed some of our strongest lenses occurred with detergent added to the water.

In conclusion, the observed direction of the net force at the surface due to radiation pressure agrees with the predictions of the Minkowski momentum. In this sense it is in agreement with the experiment of Jones and Richards.⁵ This disagrees with the expectations of Burt and Peierls³ based solely on the Abraham momentum. More detailed study of the liquid surface dynamics is needed to get more quantitative results on the magnitude of the observed force. A recent anal-

ysis by Gordon,¹² prompted by this experiment, shows that the Minkowski momentum is a pseudo-momentum that gives the correct value of the observed forces on a liquid surface or a metal vane⁵ and yet does not invalidate the true Abraham momentum.

We acknowledge helpful discussions with J. A. Arnaud, E. I. Blount, J. P. Gordon, A. G. Fox, C. K. N. Patel, and R. Kompfner.

¹J. H. Poynting, *Phil. Mag.* **S6** 9, 393 (1905).

²W. Pauli, *Theory of Relativity* (Pergamon, New York, 1958), pp. 106-111 and p. 216; C. Møller, *The Theory of Relativity* (Oxford Univ. Press, London, 1962), pp. 202-206.

³M. G. Burt and R. Peierls, to be published.

⁴W. Shockley and R. P. James, *Phys. Rev. Lett.* **18**, 876 (1967).

⁵R. V. Jones and J. C. S. Richards, *Proc. Roy. Soc., Ser. A* **221**, 480 (1954).

⁶The authors thank Professor N. Rosenzweig and Professor R. Peierls for bringing these problems to their attention.

⁷See I. Brevik, *Kgl. Dan. Vidensk. Selsk., Mat.-Fys. Medd.* **37**, No. 13 (1970), for a discussion and additional references.

⁸A. V. Kats and V. M. Kontorovich, *Pis'ma Zh. Eksp. Teor. Fiz.* **9**, 192 (1969) [*JETP Lett.* **9**, 404 (1969)].

⁹J. P. Gordon *et al.*, *J. Appl. Phys.* **36**, 3 (1965).

¹⁰P. L. Kelley, *Phys. Rev. Lett.* **15**, 1005 (1965).

¹¹A. Ashkin, *Appl. Phys. Lett.* **19**, 283 (1971).

¹²J. P. Gordon, to be published.

Electroproduction of ρ and φ Mesons*

J. T. Dakin, G. J. Feldman, W. L. Lakin, † F. Martin, M. L. Perl, E. W. Petraske, ‡ and W. T. Toner§
Stanford Linear Accelerator Center, Stanford University, Stanford, California 94305

(Received 27 November 1972)

We report measurements of ρ^0 and φ electroproduction at 19.5 GeV in a wide-aperture spectrometer which detected the scattered electron and the decay products of the vector mesons. As $|q^2|$ increases, the ρ mass spectrum shape changes, the momentum-transfer distribution broadens, and the ratio of the ρ cross section to the total cross section decreases. The ratio of longitudinally to transversely polarized ρ^0 mesons is $0.45^{+0.15}_{-0.10}$ at $|q^2|=m\rho^2$, and the interference between longitudinal and transverse amplitudes is almost maximal. The relative φ -meson cross section also decreases as $|q^2|$ increases.

Many photoproduction processes can be understood by assuming that the photon couples directly to vector-meson states. By studying vector-meson electroproduction we seek to determine how this coupling evolves as the photon becomes spacelike and its polarization has longitudinal as well as transverse components. We report here a measurement of ρ electroproduction which combines high virtual-photon energies and the ability to study ρ production and decay angular correlations.¹

The ρ electroproduction reaction

$$ep \rightarrow e\pi^+\pi^- \quad (1)$$

can be regarded as an inelastic electron scatter ($e \rightarrow e\gamma^*$) followed by the virtual photoproduction of a ρ ($\gamma^*p \rightarrow \rho p$) followed by the ρ decay ($\rho \rightarrow \pi^+\pi^-$). Quantities describing the electron scatter are q^2 , the photon mass squared; ϵ , the photon polarization; and s , the c.m. energy squared in the γ^*p collision. The ρ production is characterized by t' , the four-momentum transfer squared to the

proton less its smallest possible value (t_{\min}); and ϕ_e , the azimuthal angle between the electron scatter plane and the ρ production plane. The final $\pi^+\pi^-$ system is described by its invariant mass $m_{\pi\pi}$; ϕ , the azimuthal angle between the ρ production plane and the ρ decay plane; and θ , the ρ decay polar angle. The angle $\psi \equiv \phi_e + \phi$ is the angle between the electron scatter plane and the ρ decay plane in the limit $t' \rightarrow 0$. We use the same angle conventions as Dieterle.²

The experimental apparatus, which has been described elsewhere,³ consisted of a 19.5-GeV/c electron beam incident on a hydrogen target followed by a large-aperture magnetic spectrometer. The optical chambers were triggered by an array of shower counters each time an incident electron scattered more than 30 mrad from the beam with an energy $E' \gtrsim 4$ GeV.

All of the film was measured by a flying-spot digitizer and selected samples were also measured by a conventional manual system. Scattered electrons were identified as tracks whose